Chiang Mai J. Sci. 2018; 45(1) : 462-473
http://epg.science.cmu.ac.th/ejournal/
Contributed Paper

Preparation and Properties of Activated Carbon from Palm Shell by Potassium Hydroxide Impregnation: Effects of Processing Parameters

Sathaporn Bhungthong [a], Darunee Aussawasathien*[b], Kittipong Hrimchum [b] and Sa-Nguansak Sriphalang [a]

[a] Department of Chemistry, Ubon Ratchathani Rajabhat University, Ubon Ratchathani, 34000, Thailand.

[b] Plastics Technology Lab, Polymer Research Unit, National Metal and Materials Technology Center, Pathumthani 12120, Thailand.

*Author for correspondence; e-mail: daruneea@mtec.or.th

Received: 3 July 2015
Accepted: 14 September 2016

ABSTRACT

The preparation and characterization of activated carbons (ACs) produced from palm shells, a carbonaceous agricultural solid waste, via potassium hydroxide (KOH) impregnation were studied. The effects of processing parameters: activation temperature (500-1000°C), KOH/char ratio (1:1-3:1) and activation duration (1-3 h) on the properties of the prepared ACs were investigated. These properties included yield, pore development, Brunauer-Emmett-Teller (BET) surface area (S_{BET}), iodine number, methylene blue (MB) adsorption, composition, and surface chemistry and morphology. The optimum conditions for activation were KOH/char ratio of 2:1 at a temperature of 900°C for duration of 1 h. Under these conditions, ACs with maximum S_{BET}, micropore volume (V_{μ}) and total pore volume (V_T) of 1643 $m^2 g^{-1}$, 0.899 $cm^3 g^{-1}$ and 0.978 $cm^3 g^{-1}$, respectively were obtained, with iodine number and MB adsorption of 871 and 54% respectively. Experimental results showed that it was feasible to produce ACs with a high surface area and high adsorption capability from palm shells.

Keywords: activated carbon, palm shell, chemical activation, pore development

1. INTRODUCTION

Activated carbon (AC) is a highly porous material, which is extensively used to remove a variety of pollutants such as dyes, heavy metals, pesticides and gases, due to its large specific surface area and high adsorption. It is useful in many industrial sectors such as food, pharmaceutical, chemical, oil, mining, and in the treatment of both waste and drinking water [1-2]. There are two main sources for the production of commercial ACs: coal and lignocellulosic materials. Various lignocellulosic materials can be used to produce ACs, with the most common being agricultural wastes such as coconut shells [3], corncobs [4], nutshells [5] and cotton stalks [6]. Palm shell is a cheap and

abundant agricultural by-product in tropic countries like Malaysia, Indonesia and Thailand. It is converted into a well-developed AC by thermal and chemical activation using chemical reagents such as potassium hydroxide (KOH) [7], zinc chloride ($ZnCl_2$) [8], potassium carbonate (K_2CO_3) [9] and phosphoric acid (H_3PO_4) [10]. Among these chemical reagents, KOH has been found to be one of the most effective reagents in the production of ACs from several precursors [11-14]. However, the influence of activation conditions of ACs prepared from palm shell using KOH as an activating agent has not been thoroughly investigated. Guo and Lua [7] proposed the following reaction mechanisms of char with KOH impregnation:

$$C + 2KOH \rightarrow 2K + H_2\uparrow + CO_2\uparrow \quad (1)$$
$$C + 2KOH \rightarrow 2K + H_2O\uparrow + CO\uparrow \quad (2)$$

Since the metallic potassium (K) was mobile at the activation temperature, it was intercalated to the carbon matrix. As a result, several atomic layers of carbon had widened and formed pores. In addition, secondary reactions occurred for CO_2 and H_2O gasifications:

$$CO_2 + C \rightarrow 2CO\uparrow \quad (3)$$
$$CO_2 + 2KOH \rightarrow K_2CO_3 + H_2O\uparrow \quad (4)$$
$$H_2O + C + 2KOH \rightarrow K_2CO_3 + 2H_2\uparrow \quad (5)$$
$$H_2O + C \rightarrow CO\uparrow + H_2\uparrow \quad (6)$$

K_2CO_3 prevented the sample from over burn-off, resulting in high yield and well-developed internal porosity. The overall reaction was

$$2C+4KOH\rightarrow 2K+K_2CO_3+2H_2\uparrow+CO\uparrow \quad (7)$$

The properties of ACs depend on the activation process and the nature of the raw materials. Controlled pore size and pore size distribution are necessary for the application of ACs in a specific end use. Basic knowledge of different variables during the activation is significantly important in developing the porosity of the carbon.

Methylene blue (MB) is a cationic dye, commonly used for dyeing cotton, wool and silk. It has a hazardous effect on humans and animals causing eye burns, cyanosis, convulsions, nausea and diarrhea [15]. The MB adsorption capacity of many adsorbents has been studied due to strong adsorption of MB onto solids [16]. MB is usually used as a model substance for eliminating organic contaminants and colored bodies from aqueous solution.

A series of experiments were conducted to prepare porous carbon from palm shell using KOH as an activating agent with different processing parameters of KOH/char ratio, activation temperature and activation duration. The influences of these processing parameters on the yield, pore development, chemical compositions, and surface chemistry and morphology were investigated, including iodine number and MB adsorption to evaluate the adsorptive capacity of the AC samples.

2. MATERIALS AND METHODS

2.1 Materials

Palm shells obtained from Univanich Palm Oil Public Company Limited, Krabi, Thailand were dried naturally under sun light, crushed and sieved to a size range of 0.5-1.0 mm. They were then washed carefully with deionized (DI) water and subsequently dried at 120°C for 24 h. KOH (Analytical reagent grade; Merck Co., Ltd.) was used as an activating agent. Hydrochloric acid (HCl) and MB were supplied from Sigma-Aldrich and Merck Co., Ltd. respectively. Chemicals used for iodine number measurement, including sodium

thiosulphate ($Na_2S_2O_3.5H_2O$), iodine (I_2), potassium iodide (KI), potassium iodate (KIO_3) and cassava flour were purchased from Fluka, Sigma-Aldrich, Carlo Erba, Ajax Finechem and New grade respectively. Sodium carbonate (Na_2CO_3), potassium dihydrogen phosphate (KH_2PO_4) and disodium hydrogen phosphate (Na_2HPO_4) supplied from Carlo Erba, Merck and VWR chemicals respectively were used to prepare a buffer solution for MB adsorption measurement.

2.2 Preparation of AC

Dried palm shell was initially carbonized into char at 500°C for 2 h. The char was sieved to a uniform size ranging from 0.5 to 1.0 mm, soaked in a concentrated KOH solution, oven-dried, and then activated at temperatures of 500, 600, 700, 800, 900 and 1000°C. Impregnation ratios of 1, 2 and 3 and activation duration of 1, 2 and 3 h were studied. The study of the effect of the activation parameters on the properties of ACs was divided into three steps. The first was to find the suitable activation temperature, with the impregnation ratio and activation duration fixed at 1 and 1 h respectively. The second was to find the suitable impregnation ratio at the activation temperature selected from the first step with the activation duration constant at 1 h. The last step was to find the suitable activation duration at activation temperature and impregnation ratio selected from the first and second steps respectively.

Fifty grams of raw material was measured into a crucible boat, then placed in a horizontal alumina tube and heated in a furnace at the rate of 10°C min^{-1} from room temperature to 500°C, and maintained at this temperature for 2 h under atmosphere. The obtained char was mixed with KOH pellets and 10 mL of DI water in a beaker with magnetic stirring for 2 h and then dried in an oven at 120°C for 24 h. The crucible boat containing the base impregnated char was activated in a horizontal alumina tube inside a furnace under nitrogen (N_2) flow of 100 cm^3 min^{-1} and heated at the rate of 10°C min^{-1} from room temperature to the final temperature. After cooling, the resulting mixture was washed with a 1.0 M solution of HCl, followed by hot DI water until pH ~ 6.5 to eliminate activating agent residues and other inorganic species formed during the process. The prepared AC was oven-dried at 120°C for 24 h, sieved to obtain the particle size in the range 0.5 mm to 1.0 mm, and stored in a desiccator until required for analysis.

The yield was defined as the final weight of product after the processing stages of carbonization, activation, washing and drying. The percent yield was calculated from equation (8):

$$\text{Yield (\%)} = \frac{W_f}{W_i} \times 100 \quad (8)$$

where W_f and W_i are the final char or AC dry weight (g) and the precursor (palm shell or char) dry weight (g) respectively.

2.3 Characterization Methods

The textural properties of the ACs were investigated by N_2 adsorption isotherm at 77K (-196°C) using a Quantachrome Autosorb-1-C surface area analyzer. Prior to measurement, the samples were degassed under vacuum at 350°C at a pressure of 10^{-5} Torr for 10 h. The surface area was determined from isotherm using the BET method (S_{BET}). The definitions of total pore volume (V_T), micropore volume (V_μ), mesopore volume (V_m) and average pore size (D_p) were detailed in previous reports [4]. The volume of N_2 held in the system at the highest relative pressure of 0.99 was used directly to estimate the V_T. The Dubinin-

Radushkevich (DR) equation was used to estimate the V_μ [17-18]. The V_m was calculated as the difference between V_T and V_μ and the D_p was calculated using the relation $4V_T/S_{BET}$.

Scanning electron microscopy (SEM) analysis (Hitachi, SU-8030) was carried out to evaluate the development of the porosity. The thermogravimetric analyzer (TGA/SDTA851e) was used to analyze the proximate analysis and the results were expressed in terms of volatile matter, fixed carbon and ash content [19]. Elemental analysis was performed using an elemental analyzer (LecoTruSpec® CHN (micro)) to obtain the carbon (C), hydrogen (H), nitrogen (N), sulphur (S) and oxygen (O) contents. The chemical functionalities of the palm shell, char and AC were studied by Fourier transform infrared spectroscopy (FT-IR). The FTIR spectra were recorded at a resolution of 4 cm^{-1} with 20 scans min^{-1} between 4000 and 400 cm^{-1} using a Perkin Elmer System 2000.

2.4 Procedures for Adsorption Studies

The MB concentrations in the supernatant solutions before and after adsorption were determined using a UV-vis spectrometer (Perkin Elmer, Lambda 950) at maximum wavelength (l) of 664 nm. The MB concentration was determined by comparing absorbance to a previously obtained calibration curve. All experiments were duplicated and only the mean values were reported. The amount of MB adsorbed onto AC was calculated using equation (9):

$$MB\ adsorption\ (\%) = \frac{(C_o - C_e) \times 100}{C_o} \qquad (9)$$

where C_o and C_e (mg L^{-1}) are the initial and equilibrium liquid-phase concentrations of MB respectively.

A stock solution of 1.0 g L^{-1} was prepared by dissolving the appropriate amount of MB in 100 mL and completing the volume of 1000 mL with buffer solution (pH = 7). Batch adsorption was performed in a set of 50 mL glass bottle containing 25 mL of MB solutions with various initial concentrations (5, 10, 15, 20, and 25 mg L^{-1}) to prepare the calibration curve. An AC weight of 0.025 g was added to 25 mg L^{-1} of MB solution and then stirred at room temperature for 12 h. All samples were filtered using 0.45 mm membrane filters prior to analysis to separate the AC from MB solution and minimize the interference of small AC particles. Iodine number measurement was determined by following the ASTM D4607-86 standard.

3. RESULTS AND DISCUSSION

3.1 Yield

Relatively high yields of final products are expected in manufacturing commercial ACs. The yield values of char and ACs based on the original weight of the raw material are shown in Table 1. When activation temperature was increased a decreasing in yield was observed as a result of burn-off of carbon contents via a C-KOH reaction. The decrease in the yield for ACs is justified by reaction with the dehydrating agent (KOH), providing elimination and dehydration reactions, breaking the C-O-C and C-C bonds of the raw material [20]. A relatively high activation temperature was required for pure chemical activation as indicated by lesser weight losses at low temperatures of 500, 600 and 700°C, but a higher temperature of 900°C resulted in insignificant change compared to that of 800°C, except for 1000°C. A similar trend of decreasing in yield occurred when the KOH/char ratio and activation duration were increased. The greater the amount of KOH and the longer the activation duration, the more

direct reaction between carbon and KOH would be. Results indicated that a decrease in the yield value was significantly affected by the increase in the activation temperature and the impregnation ratio, respectively, while the activation duration had little effect on the AC yield.

Table 1. Textural characteristics of the char and ACs prepared under different activation conditions.

Sample [a]	Yield (%)	S_{BET} ($m^2 g^{-1}$)	D_p (nm)	V_μ ($cm^3 g^{-1}$)	V_m ($cm^3 g^{-1}$)	V_T ($cm^3 g^{-1}$)
Char	35.6	16	5.56	0.009	0.008	0.022
AC 500-1-1	26.9	214	4.88	0.117	0.144	0.261
AC 600-1-1	26.4	356	2.64	0.195	0.040	0.235
AC 700-1-1	26.1	631	2.39	0.345	0.032	0.377
AC 800-1-1	22.2	1014	2.34	0.555	0.038	0.593
AC 900-1-1	22.0	1305	2.43	0.715	0.077	0.792
AC 1000-1-1	19.8	1262	2.41	0.691	0.067	0.758
AC 900-2-1	21.2	1643	2.38	0.899	0.079	0.978
AC 900-3-1	18.7	1623	2.38	0.890	0.075	0.965
AC 900-2-2	20.9	1441	2.49	0.792	0.104	0.896
AC 900-2-3	20.2	1373	2.36	0.754	0.056	0.810

[a]*Note:* AC a-b-c denotes AC activation temperature (°C)-KOH/char ratio-activation duration (h).

3.2 Textural Characterization

Table 1 presents the physical properties of the char and ACs derived from palm shell by KOH activation. The activation process rearranges the carbon structure producing a more ordered structural skeleton. The pore development occurs in four stages: (I) opening of previously accessible pores, (II) creation of new pores, (III) widening of the existing pores and (IV) combination of the existing pores due to pore wall breakage [21].

The S_{BET} of ACs increased when the activation temperature increased from 500°C to 900°C, and then dropped at 1000°C. The maximum S_{BET}, V_μ and V_T values were obtained from the AC prepared at 900°C. Therefore, the activation temperature of 900°C was selected for further study of the impregnation ratio and activation duration effects on the AC properties. This progressive activation temperature increased the C-KOH reaction rate, resulting in high carbon burn-off. Simultaneously, the volatiles from the sample continued to evolve with increasing activation temperature. The devolatilization process further developed the rudimentary pore structure in the char, whereas the C-KOH reaction enhanced the existing pores and created new porosities [22]. At low activation temperature, 500°C, 600°C and 700°C, the S_{BET} increased insignificantly compared to char. This is because of the insufficient heat to melt KOH to cover the entire surface of the carbon, resulting in physical pyrolysis on the carbon surfaces. The decrease of S_{BET} at high activation temperature of 1000°C resulted from the continued etching of KOH on the carbon surfaces which damaged the pore structure (proved by SEM observation section).

The surface area of ACs increased with increasing impregnation ratio from 1 to 2 and then slightly decreased at 3. Therefore, the impregnation ratio of 2 was selected for the study of the activation duration effect on the AC properties. The agent/char ratio has been found to be the most important parameter in a chemical activation process to obtain ACs with high surface area [23-24]. Higher activating agent concentrations consistently yielded products with a much larger external surface area as well as large V_μ [25]. The S_{BET} of ACs tended to decrease when the activation duration was raised. At long activation duration, the pore structure might be blocked by small debris particles on the surface of the AC due to the excessive etching by KOH. This phenomenon can lead to a reduction in the accessible area, thus resulting in a decrease in S_{BET} [26].

The V_T is directly related to the development of porosity of the material with micropores responsible for the increase of V_T. The presence of mesopores and micropores in ACs enhances their adsorption capacities, especially for large molecules of adsorbates as dye molecules [27]. The V_μ and V_T steadily increased with activation temperature from 500°C to 900°C and then slightly decreased at 1000°C. The V_m tended to decrease as the activation temperature increased from 500-800°C but increased suddenly at 900°C, and then slightly dropped at 1000°C. This feature can be utilized to control the mesopore volume of the high surface AC in the production process. The V_μ, V_m and V_T progressively increased with increasing impregnation ratio from 1 to 2 h, and then slightly dropped at 3 h. With higher impregnation ratios, the weight losses were due to the increasing release of volatile products as a result of intensifying dehydration and elimination reactions [25]. The part of the process in which micropores kept increasing in this range of agent/char ratios is called the micropore development stage. Simultaneously, the micropores were widened into mesopores, called the pore-volume-expanding stage. The V_T reduction is indicative of a pore blockage or a structure collapse by increasing the chemical ratio, thus resulting in a smaller internal volume [28]. At low temperature and impregnation ratio, the pore structure mainly consisted of micropore. However, as the temperature and impregnation ratio increased, the creation of micropore structure and widening of micropores to mesopores also increased, resulting in the increase of the V_T of AC [29-30]. The V_μ, V_m and V_T decreased with activation duration increase from 1 to 3 h, which were in good agreement with the S_{BET} results. The activation temperature, impregnation ratio and activation duration all had a significant effect on the pore structure of AC produced. Most of the pores had sizes mostly in the range of 2.34-4.88 nm for prepared AC samples, indicating a development of microporosity in the material.

3.3 N_2 Adsorption Isotherm and Pore Size Distribution

Several previous research studies have utilized the adsorption of inert gases to understand the AC pore structure and determine the appropriateness for various applications. The adsorption capacity of the AC depends largely on the quantity of micropores. Hence adsorption capacity can be directly related to the micropore volume in the sample. Figure 1 (a)-(c) shows the typical adsorption/desorption isotherm of N_2 at 77 K for all ACs with different activation temperatures, impregnation ratios, and activation durations respectively. The adsorbed volume of ACs increased with increasing activation temperatures from 500°C to 900°C

and then slightly decreased at 1000°C. At too high temperature caused severe activation reaction, resulting in the conversion of micropores to meso- or even marcropore due to over burn-off. A progressive increase in N_2 volume was observed over the whole range of relative pressure for each temperature.

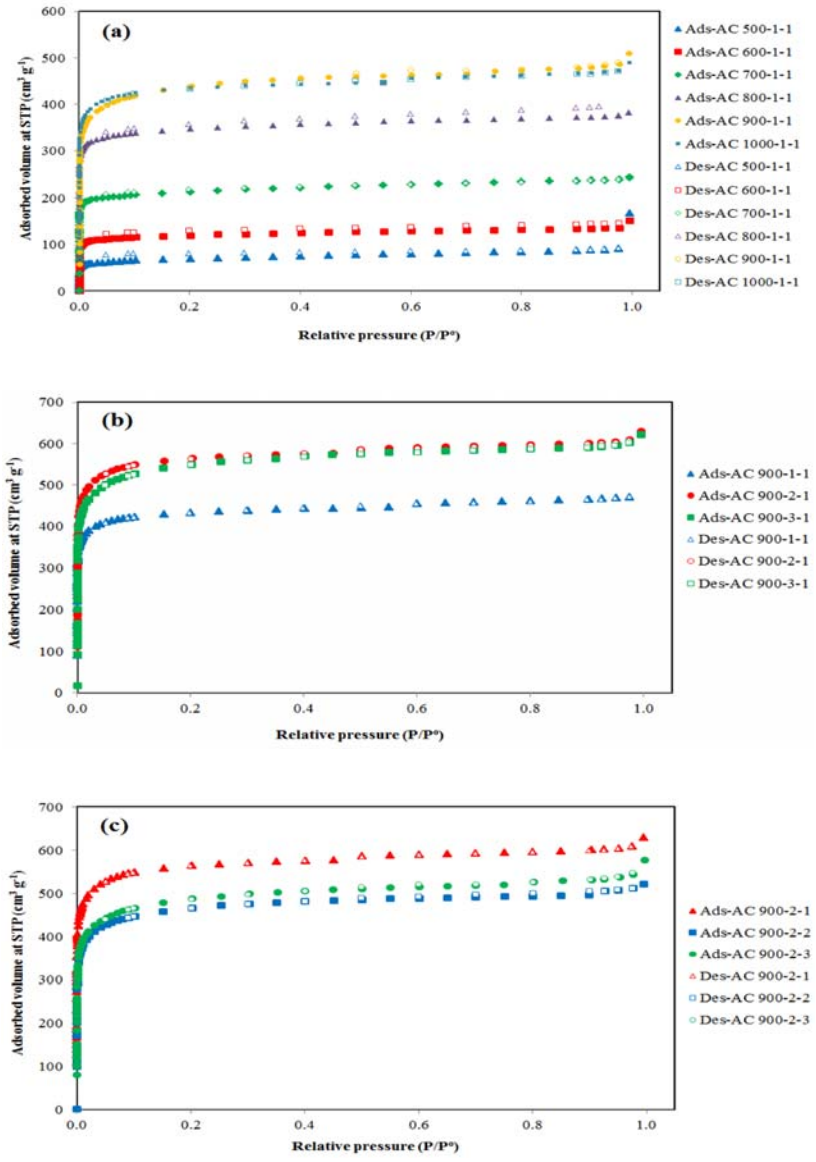

Figure 1. Adsorption/desorption isotherms of N_2 at 77 K on ACs derived from palm shell with KOH activation: (a) at different activation temperatures, (b) at different impregnation ratios, and (c) at different activation durations.

As the impregnation ratio increased from 1 to 2, the N_2 adsorbed volume increased over the whole range of relative pressure, and slightly dropped at the ratio of 3. The pore development was due to the enhanced activation reactions between carbon and activating agent at suitable temperatures. However, a higher impregnation ratio resulted in severe activation reactions that had a detrimental effect on the development of internal pores, particularly micropores. Some micropores, which accounted for the large specific surface area, were converted to meso- or even macropores due to excessive reaction of activating agent. For the same reason, the effects of activation duration on the N_2 adsorbed volume showed a trend similar to that of impregnation ratio effect. The isotherm curves are of Type I isotherms which generally exhibit the presence of micropores [31]. Furthermore, this type of isotherm indicates that the adsorbate and adsorbent have a high affinity and that the material consists mostly of micropores, with higher initial volume shown for the AC prepared at the impregnation ratio of 2 at 900°C for 1 h. The effects of activation conditions on the N_2 adsorbed volume corresponded to the V_μ, V_T and S_{BET} results.

3.4 SEM Observations

Figure 2 (a) and (b) shows SEM images of the palm shell and char. There were no pores on the palm shell surface, whereas a small number of pores were seen on the char surface. Figure 3 shows the SEM images of the ACs prepared under different activation temperatures, KOH/char ratios and activation durations. The ACs had several cavities and pores with different sizes and shapes compared to palm shell and char. The pores and cavities resulted from the release of volatile components and the evaporation of KOH from the spaces that were previously occupied by the KOH [32-33]. At high temperatures of 900°C, rough surfaces were produced beside the micropores with more irregular shaped pores, leading to higher surface areas than the ACs prepared at lower temperatures of 500°C to 800°C. At high activation temperature of 1000°C, high impregnation ratio of 3 and long activation duration of 2 and 3, there were also a large number of small and large holes with crevices and cracks on the surface of the ACs and the pore structures were partially filled with debris particles produced by the etching of KOH, resulting in lower surface area and total pore volume.

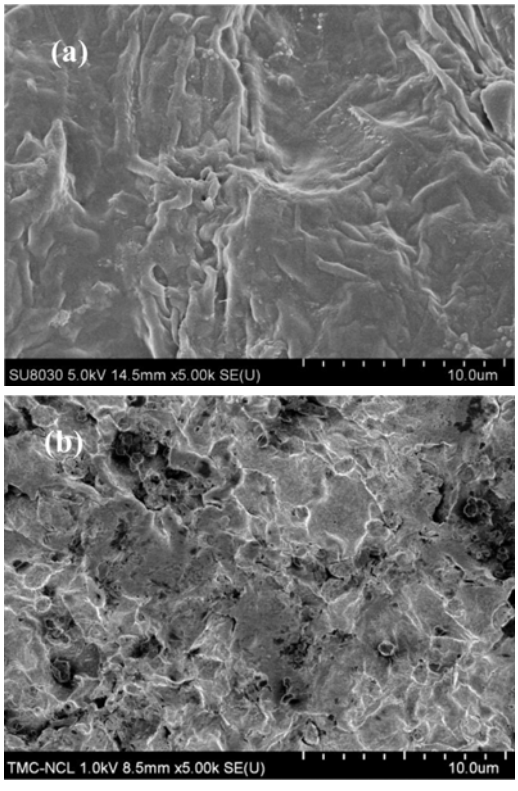

Figure 2. SEM photographs of (a) palm shell and (b) char.

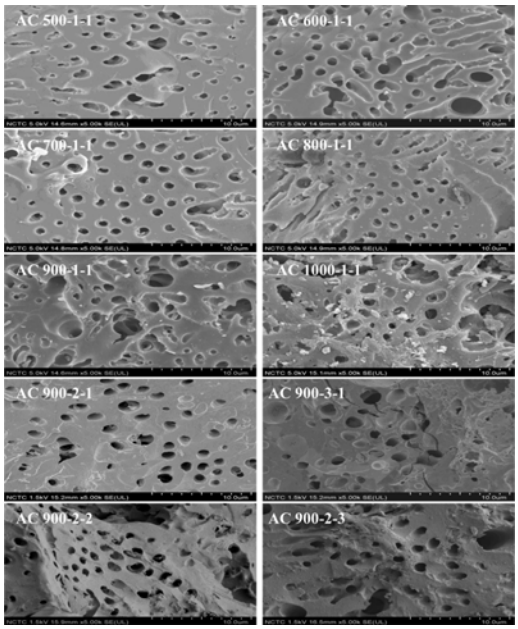

Figure 3. SEM photographs of prepared ACs under different activation conditions.

3.5 Chemical Adsorption Properties

The most important property of the AC is its adsorptive capacity which is closely related to the specific surface area. Typically, the higher the surface area of the AC, the greater its adsorptive capacity [34]. Iodine number mainly relates to the micropore structure of the AC, whereas MB adsorption involves the mesopore structure. The iodine number and MB adsorption results of prepared ACs corresponded to the S_{BET}, V_{μ}, V_T and SEM results. The iodine number and MB adsorption of ACs increased from 113-499 mg g^{-1} and 16-50% respectively when the activation temperature increased from 500-900°C, and then dropped to 468 mg g^{-1} and 47% at 1000°C (Figure 4 (a)). As the impregnation ratio increased from 1 to 2, the iodine number increased from 499-871 mg g^{-1}, and then slightly dropped to 852 mg g^{-1} at the impregnation ratio of 3 (Figure 4 (b)). The MB adsorption increased from 50% to 59% as the impregnation ratio increased from 1 to 3. The iodine number and MB adsorption of ACs decreased from 871-703 mg g^{-1} and 54-51% respectively as the activation duration was raised from 1 to 3 h (Figure 4 (c)).

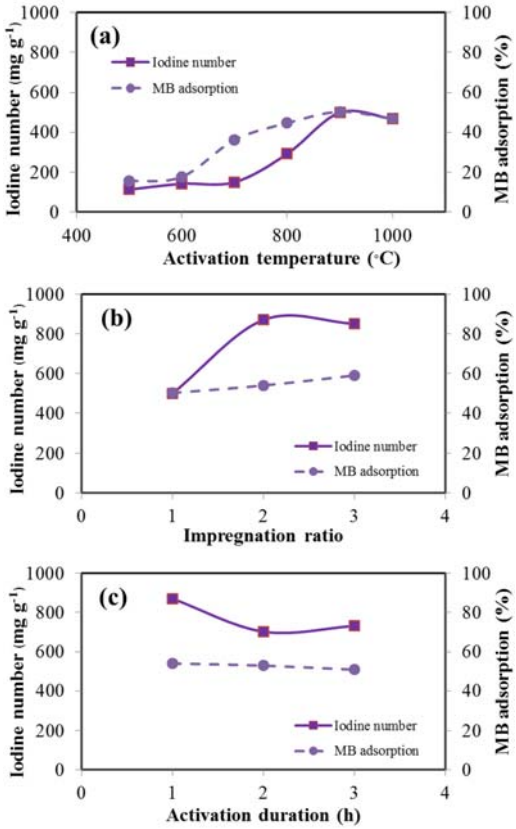

Figure 4. Iodine number and MB adsorption of ACs prepared under different activation conditions.

3.6 Chemical Surface Characterization

Elemental compositions of the palm shell, char and AC were determined. This is helpful for understanding the activation mechanism and the functional appearance of various applications, such as surface functional groups of adsorption and conductivity of supercapacitors. Table 2 shows the volatile, fixed carbon and ash contents by weight from proximate analysis and chemical compositions (C, H, N, S, and O) according to elemental analysis of the palm shell, char and AC. The volatile content

of the char and AC dramatically decreased, whereas the fixed carbon and ash amount increased after the carbonization and activation processes. The carbon contents of char and AC increased compared with palm shell after heat treatment, while the oxygen content decreased. The proximate analysis was in good agreement with the elemental composition results. The chemical C content of the palm shell was lower than that of char and AC. Therefore, the C content increased, while the oxygen content largely decreased after the carbonization and activation processes. These results concur with previous studies [35]. FT-IR spectra were obtained to qualitatively evaluate the chemical structures of the palm shell, char and AC (Figure 5). The FT-IR spectrum of the palm shell (Figure 5 (a)), indicates various surface functional groups. The broad band at 3350-3450 cm^{-1} is typically attributed to hydroxyl groups. The band located at 2800-2950 cm^{-1} corresponds to C-H stretching vibration. The region 1650-1750 cm^{-1} is attributed to axial deformation of carbonyl groups (C=O). The stretching vibration of the molecular plane of C=C bonds in the aromatic rings appears between 1540-1580 cm^{-1}. The broad band at 1050-1200 cm^{-1} is attributed to alcoholic (C-OH stretching) and ether (R-O-R) groups. The band caused by cyclic groups is located at 650-880 cm^{-1}. The presence of hydroxyl groups, carbonyl groups, ethers and aromatic compounds is evidence of the lignocellulosic structure of palm shell, also observed in others materials such as Tunisian olive-waste cakes [36], jackfruit peel waste [37] and cotton stalks [38]. Adinata et al. [9] also reported that the palm shell was mainly composed of cellulose, halocellulose and lignin. Figure 5 (b) shows the FT-IR spectrum of the char, exhibiting the disappearance of bands at 3350-3450 cm^{-1} and 2800-2950 cm^{-1}. Other regions at 1650-1750 cm^{-1}, 1540-1580 cm^{-1}, 1050-1200 $cm^{-1}$and 650-880 cm^{-1} decreased drastically, indicating a decrease in the functionality of the raw material. The FT-IR spectrum of the AC 900-2-1 (Figure 5 (c)) shows the disappearance of bands compared to the palm shell and char spectra, indicating that the chemical bonds were completely broken during the carbonization and activation processes.

Table 2. Proximate and elemental analyzes of the palm shell, char and AC 900-2-1.

Material	Volatile (wt%)	Fixed carbon (wt%)	Ash (wt%)	C (wt%)	H (wt%)	N (wt%)	O (wt%)	S (wt%)
Palm shell	70.0	29.1	0.9	51.4	6.1	0	41.8	0.7
Char	11.8	81.6	6.6	78.9	2.9	0	17.5	0.7
AC 900-2-1	14.0	84.0	2.0	78.1	0	0	21.2	0.7

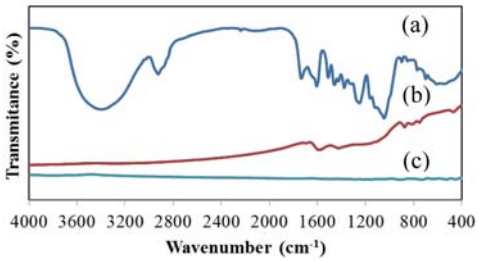

Figure 5. FT-IR spectra of (a) palm shell, (b) char and (c) AC 900-2-1.

4. CONCLUSIONS

Palm shell was used to prepare ACs via a chemical activation process, using KOH as the activating agent. The impregnation ratio had a greater impact on the AC properties than the activation temperature and activation duration respectively. The properties of AC prepared with an impregnation ratio of 2 at 900°C for 1 h attained a maximum

value of S_{BET}, V_{μ} and V_T with high iodine number and MB adsorption. The chemical and textural characteristics of the palm shell AC obtained from this study showed a potential application in chemical adsorption treatments. The comparative study of adsorption equilibrium and kinetics of MB onto ACs will be further investigated using ACs prepared from palm shell by NaOH and KOH impregnation methods with optimum properties.

ACKNOWLEDGEMENTS

The authors acknowledge the National Science and Technology Development Agency (NSTDA) for senior project scholarship 2014 (SP-57-MT09) under the Young Scientist and Technologist Program (YSTP).

REFERENCES

[1] Crini G., *Bioresour. Technol.*, 2006; **97**: 1061-1085.

[2] Saipanya S. and Saralmonsri T., *Chiang Mai J. Sci.*, 2010; **37**: 99-105.

[3] Cazetta A., Vargas A.M.M., Nogami E.M., Kunita M.H., Guilherme M.R., Martins A.C., Silva T.L., Moraes J.C.G. and Almeida V.C., *Chem. Eng. J.*, 2011; **174**: 117-125.

[4] Tseng R.L., *J. Colloid Interf. Sci.*, 2006; **303**: 494-502.

[5] Hayashi J., Horikawa T., Takeda I., Muroyama K. and Ani F.N., *Carbon*, 2002; **40**: 2381-2386.

[6] Deng H., Li G., Yang H. and Tang J., *Chem. Eng. J.*, 2010; **163**: 373-381.

[7] Guo J. and Lua A.C., *J. Colloid Interf. Sci.*, 2002; **254**: 227-233.

[8] Hesas R.H., Arami-Niya A., Daud W.M.A.W. and Sahu J.N., *J. Anal. Appl. Pyrol.*, 2013; **104**: 176-184.

[9] Adinata D., Daud W.M.A.W. and Aroua M.K., *Bioresour. Technol.*, 2007; **98**: 145-149.

[10] Guo J. and Lua A.C., *Mater. Chem. Phys.*, 2003; **80**: 114-119.

[11] Ahmadpour A. and Do D.D., *Carbon*, 1996; **34**: 471-479.

[12] Otowa T., Yamada M., Tanibata R. and Kawakami M., *Proceedings of the International Symposium on Gas Separation Technology*, Antwerp, Belgium, 10-15 September 1989; 263.

[13] Otowa T., Nojima Y. and Miyazaki T., *Carbon*, 1997; **35**: 1315-1319.

[14] Hu Z. and Srinivasan M.P., *Micropor. Mesopor. Mat.*, 1999; **27**: 11-18.

[15] Senthilkumaar S., Varadarajan P.R., Porkodi K. and Subbhuraam C.V., *J. Colloid Interf. Sci.*, 2005; **284**: 78-82.

[16] Hameed B.H., Din A.T.M. and Ahmad A.L., *J. Hazard. Mater.*, 2007; **141**: 819-825.

[17] Rouquerol F., Rouquerol J. and Sing K., Assessment of Surface Area; in Rouquerol J., Rouquerol F. and Sing K., eds., *Adsorption by Powders and Porous Solids: Principles, Methodology and Applications*, Academic Press, London, 1999: 165-189.

[18] Barrett E.P., Joyner L.G. and Halenda P.P., *J. Am. Chem. Soc.*, 1951; **73**: 373-380.

[19] Lua A.C. and Guo J., *Carbon*, 1998; **36**: 1663-1670.

[20] Basta A.H., Fierro V., El-Saied H. and Celzard A., *Bioresour. Technol.*, 2009; **100**: 3941-3947.

[21] Yang K., Peng J., Srinivasakannan C., Zhang L., Xia H. and Duan X., *Bioresour. Technol.*, 2010; **101**: 6163-6169.

[22] Hayashi J., Horikawa T., Muroyama K. and Gomes V.G., *Micropor. Mesopor. Mat.*, 2002; **55**: 63-68.

[23] Ahmadpour A. and Duong D.D., *Carbon*, 1997; **35**: 1723-1732.

[24] Caturla F., Molina-Sabio M. and Rodriguez-Reinoso F., *Carbon*, 1991; **29**: 999-1007.

[25] Evans M.J.B., Halliop E. and MacDonald J.A.F., *Carbon*, 1999; **37**: 269-274.

[26] Li W., Zhang L.B., Peng J.H., Li N. and Zhu X.Y., *Ind. Crop. Prod.*, 2008; **27**: 341-347.

[27] Hartono S.B., Ismadji S., Sudaryanto Y. and Irawaty W., *J. Ind. Eng. Chem.*, 2005; **11**: 864-869.

[28] Foo K.Y. and Hameed B.H., *Bioresour. Technol.*, 2012; **103**: 398-404.

[29] Ismadji S. and Bhatia S.K., *Langmuir*, 2000; **16**: 9303-9313.

[30] Ismadji S. and Bhatia S.K., *Langmuir*, 2001; **17**: 1488-1498.

[31] Brum S.S., Bianch M.L., Silva V.L., Gonclaves M., Guerreiro M.C. and Oliveira L.C.A., *Quim. Nova*, 2008; **5**: 1048-1052.

[32] Maldhure A.V. and Ekhe J.D., *Chem. Eng. J.*, 2011; **168**: 1103-1111.

[33] Deng H., Zhang G., Xu X., Tao G. and Dai J., *J. Hazard. Mater.,* 2010; **182**: 217-224.

[34] Kenneth N.E., Gounaris V. and Hou W.S., *Adsorption Technology for Air and Water Pollution Control.*, Lewis, Chelsea MI, 1992.

[35] Minkova V., Marinov S.P., Zanzi R. and Bjornbom B.T., *Micropor. Mesopor. Mat.*, 2002; **55**: 63-68.

[36] Baccar R., Bouzid J., Feki M. and Montiel A., *J. Hazard. Mater.*, 2009; **162**: 1522-1529.

[37] Prahas D., Kartika Y., Indraswati N. and Ismadji S., *Chem. Eng. J.*, 2008; **140**: 32-42.

[38] El-Hendawy A.A., Alexander A.J., Andrews R.J. and Forrest G., *J. Anal. Appl. Pyrol.*, 2008; **82**: 272-278.